An FDTD Algorithm with Perfectly Matched Layers for General Dispersive Media

Guo-Xin Fan, *Member, IEEE,* and Qing Huo Liu, *Senior Member, IEEE*

***Abstract*—A three-dimensional (3-D) finite-difference time-domain (FDTD) algorithm with perfectly matched layer (PML) absorbing boundary condition (ABC) is presented for general inhomogeneous, dispersive, conductive media. The modified time-domain Maxwell's equations for dispersive media are expressed in terms of coordinate-stretching variables. We extend the recursive convolution (RC) and piecewise linear recursive convolution (PLRC) approaches to arbitrary dispersive media in a more general form. The algorithm is tested for homogeneous and inhomogeneous media with three typical kinds of dispersive media, i.e., Lorentz medium, unmagnetized plasma, and Debye medium. Excellent agreement between the FDTD results and analytical solutions is obtained for all testing cases with both RC and PLRC approaches. We demonstrate the applications of the algorithm with several examples in subsurface radar detection of mine-like objects, cylinders, and spheres buried in a dispersive half-space and the mapping of a curved interface. Because of their generality, the algorithm and computer program can be used to model biological materials, artificial dielectrics, optical materials, and other dispersive media.**

***Index Terms*—Dispersive medium, finite-difference time-domain (FDTD) method, ground-penetrating radar (GPR), perfectly matched layer (PML), plasma, transient wave scattering.**

I. Introduction

FINITE-DIFFERENCE time-domain (FDTD) method, as one of most powerful computational methods in electromagnetics, has been widely used to model the wave propagation, scattering, and radiation since it was first introduced by Yee [1] in 1966. In the early development and application of FDTD, the parameters of media are constants independent of frequency. When the media are frequency dependent, especially for those encountered in the applications involving earth, biological materials, artificial dielectrics, optical materials, this frequency dispersive property will significantly change the electromagnetic response in the media. In these cases, the original FDTD algorithm needs to be modified to account for the frequency dispersion of the media.

For media dispersive only electrically (i.e., magnetically nondispersive), an important issue in the frequency-dependent FDTD methods is how to calculate efficiently the temporal convolution of the electric field with causal susceptibility in an explicit or implicit form. Up until now, three major frequency-dependent FDTD methods have been proposed: recursive convolution (RC) [2]–[8], auxiliary differential equation (ADE) [9]–[13], and Z-transform (ZT) [14], [15].

In the RC approach, the convolution integral is discretized into convolution summation which is then evaluated recursively. This approach has been used to model various dispersive media such as Debye media [2], [7], [8], unmagnetized plasma [3], Nth-order Lorentz media [4], and general media [5]. Recently, a modified version of RC, the piecewise linear recursive convolution (PLRC) was presented by introducing a piecewise linear approximation (in contrast to the piecewise constant approximation in RC approach) to the electric field in the convolution integrals and was applied to lower order Lorentz and Debye media [6].

In the ADE method, either the frequency-domain constitutive relation between the electric flux density and electric field or the time-domain convolution integral is first expressed by ordinary differential equations, which are then discretized into difference equations [10], [13]. The ADE approach was used to model Debye media [9]–[11], Lorentz media [9], [10], and Nth-order Lorentz media [13].

In the ZT approach, the time-domain convolution integral is reduced to a multiplication using the Z-transform, and a recursive relation between electric flux density and electric field is derived. The ZT approach was applied to Debye, unmagnetized plasma, and Lorentz media [14], [15].

It is reported that among all the above frequency-dependent FDTD methods, the RC and PLRC methods require least

TABLE I
PARAMETERS FOR LORENTZ MEDIA.

Medium I	Medium II
$\epsilon_\infty = 4$	$\epsilon_\infty = 1.5$
$\epsilon_s = 8$	$\epsilon_s = 3.5$
$\omega_1 = 2\pi \times 10^7$ rad/s	$\omega_1 = 1.2 \times 2\pi \times 10^7$ rad/s
$\omega_2 = 2.5 \times 2\pi \times 10^7$ rad/s	$\omega_2 = 2.8 \times 2\pi \times 10^7$ rad/s
$\delta_1 = 0.1\omega_1$	$\delta_1 = 0.1\omega_1$
$\delta_2 = 0.1\omega_2$	$\delta_2 = 0.1\omega_2$
$G_1 = 0.4$	$G_1 = 0.5$
$G_2 = 0.6$	$G_2 = 0.5$
$\sigma = 2 \times 10^{-4}$ S/m	$\sigma = 5 \times 10^{-5}$ S/m

Manuscript received November 18, 1997; revised October 8, 1999. This work was supported by Sandia National Laboratories under an SURP Grant, by the Environmental Protection Agency under PECASE Grant CR-825–225–010, and by the NSF under CAREER Grant ECS-9702195.

The authors were with the Klipsch School of Electrical and Computer Engineering, New Mexico State University, Las Cruces, NM 88003 USA. They are now with the Department of Electrical and Computer Engineering, Duke University, Durham, NC 27708-0291 USA (email: Qing.Liu@duke.edu).

Publisher Item Identifier S 0018-926X(00)02455-8.

0018–926X/00$10.00 © 2000 IEEE

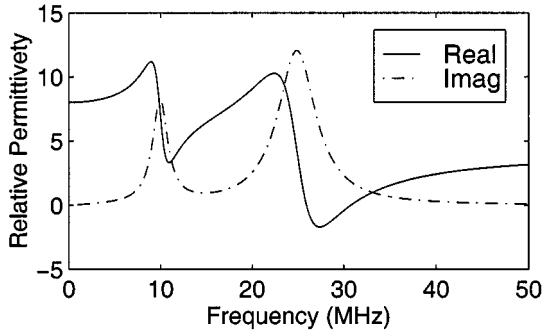

(a)

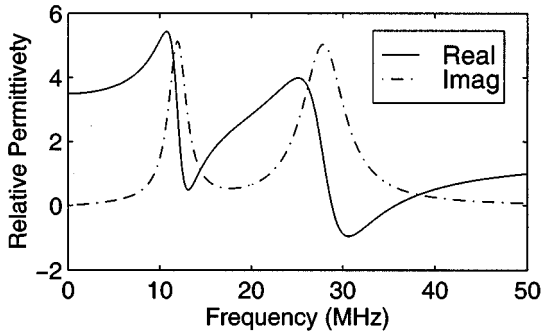

(b)

Fig. 1. Complex permittivity of (a) Lorentz media I and (b) Lorentz media II.

computer storage, and the PLRC, ADE, and ZT approaches have better accuracy than the RC approach [6]. In addition, the RC and PLRC approaches allow a unified treatment of a wide variety of dispersive media, while the ADE and ZT approaches require the different formulations for different types of dispersive media. A recent advance in the ADE approach reduces its storage requirement to the same amount as in the RC approach by using the state equation description [12]. The formulations are given for the Nth-order Lorentz media and Mth-order Debye media in different forms. More recently, a general FDTD algorithm for dispersive media was proposed in two forms using Padé approximation of either the complex frequency-dependent permittivity or conductivity in the Z-transform space. Because of the flexibility of Padé approximation, this algorithm can model arbitrary dispersive media [16]. However, it needs slightly more storage than the PC and PLRC approaches.

As in the FDTD method for nondispersive media, when applied to unbounded media, the frequency-dependent FDTD algorithm calls for absorbing boundary conditions (ABC's) in order to truncate the computational domain. The conventional ABC's fall into two categories: differential-based ABC's [17]–[22] and material-based ABC's [23]–[26]. The former is not well suited for parallel computation, while the latter provides zero reflection at the absorbing boundary only at normal incidence and is angle and frequency dependent. Other new ABC's such as superabsorption [27], measured equation of invariance (MEI) [28], numerical ABC's [29], and complementary operator [30] can be used to truncate the computation region more effectively, but are mainly used for scattering problems in free-space. The previous FDTD algorithms on

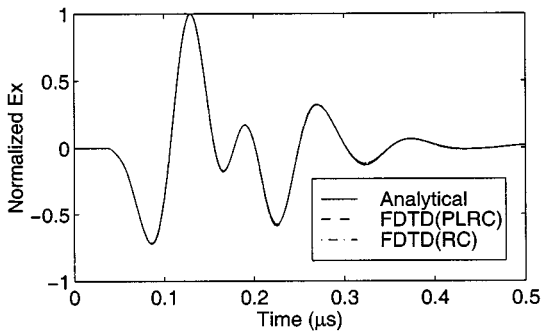

Fig. 2. Comparison of FDTD results (the E_x component at the fourth receiver) with analytical solutions for homogeneous Lorentz medium I.

dispersive media employed the differential-based ABC's such as Mur's ABC and Liao's ABC. Recently, Berenger introduced a highly effective ABC, the perfectly matched layer (PML), which gives zero reflection at the absorbing boundary for all frequencies and all angles of incidence [31]. As a material ABC, the PML is ideal for parallel computation. In addition, the PML ABC can be applied to the domain where a curved interface exists. All these properties of PML are without rivals of all previous ABC's. As a nonphysical absorbing medium, the PML has been given different interpretations with various different formulations [32]–[35]. So far, most PML ABC's are applied to lossless and nondispersive media.

Recently, the PML ABC has been extended to nondispersive lossy media (i.e., ϵ and σ are independent of frequency) with different formulations [36], [37], and a FDTD algorithm and application examples are given in [37]. A uniaxial PML method combined with the ADE approach in the FDTD algorithm is extended to lossy and dispersive media and the formulation for Lorentz media is given [38]. An ABC based on PML is presented for the spatially uniform Debye and Lorentz dispersive media in [39] and for inhomogeneous Debye and Lorentz media using stretched coordinates in [40].

In this paper, a three-dimensional (3-D) FDTD algorithm is presented for general inhomogeneous, dispersive, conductive media using the coordinate stretching approach and the RC and PLRC approaches are extended to general dispersive media in a more unified form. Three types of dispersive media, i.e., Lorentz media, Debye media, and unmagnetized plasma, are treated as special cases of our general formulas. Section II develops the formulation of the algorithm. Section III shows several examples for validation and applications.

II. Formulation

A. Modified Maxwell's Equations for Dispersive Media

Consider an isotropic, conductive, inhomogeneous, linear permittivity dispersive medium. Using the coordinate stretching approach [32], the modified Maxwell's curl equations in the frequency domain can be written as

$$\nabla_e \times \mathbf{E} = i\omega\mu\mathbf{H} - \mathbf{M} \tag{1}$$

$$\nabla_e \times \mathbf{H} = -i\omega\mathbf{D} + \sigma\mathbf{E} + \mathbf{J} \tag{2}$$

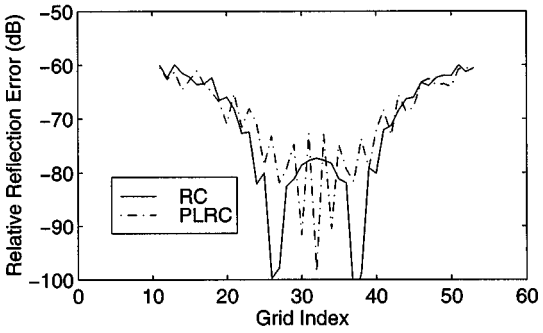

Fig. 3. Relative reflection error from the PML boundary $(n = 1000)$.

where a time dependence of $e^{-i\omega t}$ is implied. The operator ∇_e expressed in terms of the complex coordinate-stretching variables e_η $(\eta = x, y, z)$ is

$$\nabla_e = \sum_{\eta=x,y,z} \hat{\eta} \frac{1}{e_\eta} \frac{\partial}{\partial \eta}. \tag{3}$$

For a general medium, the complex coordinate-stretching variable is chosen as [37]

$$e_\eta = a_\eta + i\frac{\omega_\eta}{\omega} \tag{4}$$

where a_η and ω_η are frequency independent within the frequency band of interest.

Following [32], all the fields and sources $\mathbf{E}, \mathbf{D}, \mathbf{H}, \mathbf{J}$ and $\mathbf{M}$ are split in the following forms:

$$\mathbf{E} = \sum_{\eta=x,y,z} \sum_{\substack{\zeta=x,y,z \\ \zeta\neq\eta}} \hat{\zeta} E_\zeta^{(\eta)}. \tag{5}$$

Equations (1) and (2) can then be converted into time domain for the split fields $(\eta = x, y, z)$

$$a_\eta \mu \frac{\partial \mathbf{H}^{(\eta)}}{\partial t} + \mu\omega_\eta \mathbf{H}^{(\eta)} = -\frac{\partial}{\partial \eta}(\hat{\eta} \times \mathbf{E}) - \mathbf{M}^{(\eta)} \tag{6}$$

$$a_\eta \frac{\partial \mathbf{D}^{(\eta)}}{\partial t} + \omega_\eta \mathbf{D}^{(\eta)} + a_\eta \sigma \mathbf{E}^{(\eta)} + \omega_\eta \sigma \int_{-\infty}^{t} \mathbf{E}^{(\eta)}\, dt = \frac{\partial}{\partial \eta}(\hat{\eta} \times \mathbf{H}) - \mathbf{J}^{(\eta)}. \tag{7}$$

Equations (6) and (7) consist of a total of 12 scalar equations since both $\mathbf{E}^{(\eta)}$ and $\mathbf{H}^{(\eta)}$ have two scalar components perpendicular to $\hat{\eta}$ and $\mathbf{D}^{(\eta)}$ also has the two corresponding components due to the constitutive relations of the media. These equations are insufficient to solve the total 18 field components. The remaining equations will be given by the constitutive relations as discussed in the next subsection.

In passing, note that with the introduction of PML, there is an additional term involving the time-integrated electric field in (7). As pointed out by [37], this term represents the coupling of the loss in PML with the regular conduction loss.

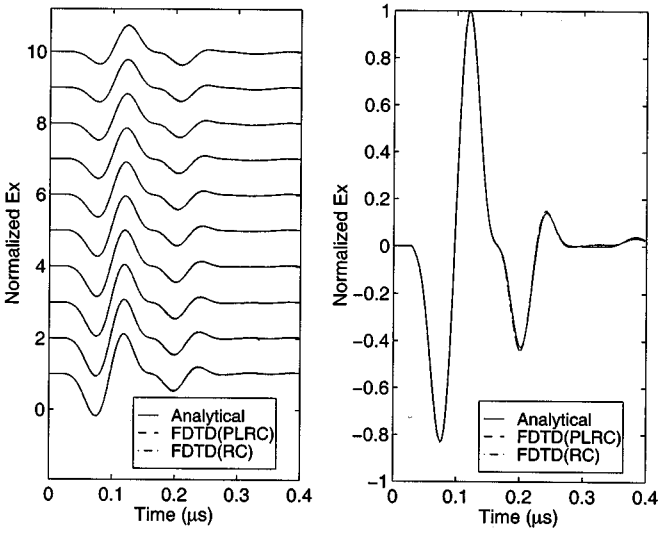

Fig. 4. Comparison of FDTD results with analytical solutions for a Lorentz sphere (medium I) in a homogeneous Lorentz medium I.

B. Recursive Convolution Approaches

Noting that the constitutive relation takes the same form for all split components, for simplicity we omit all the superscript (η) in this subsection.

The relationship between the electrical flux density and the electric field intensity in the frequency domain is described by

$$\mathbf{D}(\omega) = \epsilon_0[\epsilon_\infty + \chi(\omega)]\mathbf{E}(\omega) \tag{8}$$

where ϵ_0 is the free-space permittivity, ϵ_∞ is the relative permittivity at $\omega \to \infty$, and χ is the electric susceptibility. For a linear dispersive medium, the corresponding time-domain relation can be obtained by Fourier transform as

$$\mathbf{D}(t) = \epsilon_0\epsilon_\infty \mathbf{E}(t) + \epsilon_0 \int_{-\infty}^{t} \mathbf{E}(\tau)\chi(t-\tau)\, d\tau. \tag{9}$$

Equation (9) shows a nonlocal temporal convolution relation between $\mathbf{D}$ and $\mathbf{E}$ for frequency dispersive media. It is clear that this nonlocal behavior implies a large storage for the history of $\mathbf{E}$.

Introducing discrete time steps, i.e., $t = n\triangle t$, we obtain from (9)

$$\mathbf{D}(t) \approx \mathbf{D}(n\triangle t) = \mathbf{D}(n) = \epsilon_0\epsilon_\infty \mathbf{E}(n) + \epsilon_0 \int_0^{n\triangle t} \mathbf{E}(\tau)\, \chi(n\triangle t - \tau)\, d\tau \tag{10}$$

assuming $\mathbf{E}(t) = 0$ for $t < 0$. For a linear dispersive medium, the frequency-domain susceptibility functions, as the transfer function of a linear system, can generally be expressed as a ratio of two polynomials [5], [13] or as a pole-residue expansion, i.e.,

$$\chi(\omega) = \frac{\sum_{q=1}^{M'} \beta_q\, s^q}{\sum_{q=1}^{M} \zeta_q\, s^q} = \sum_{q=1}^{M} \frac{\Gamma_q}{s - s_q}, \quad (M > M') \tag{11}$$

TABLE II
PARAMETERS FOR UNMAGNETIZED PLASMA.

$\omega_p = 2.87 \times 2\pi \times 10^{10}\,\mathrm{rad/s}$	$\nu_c = 2 \times 10^{10}\,\mathrm{Hz}$

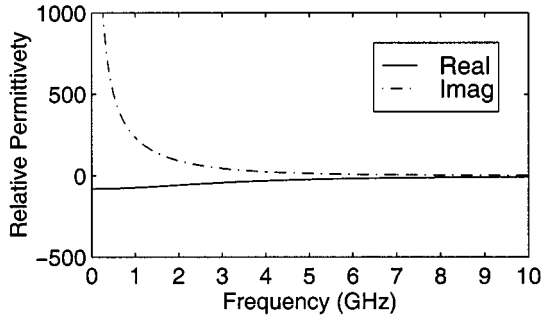

Fig. 5. Complex permittivity of the unmagnetized plasma.

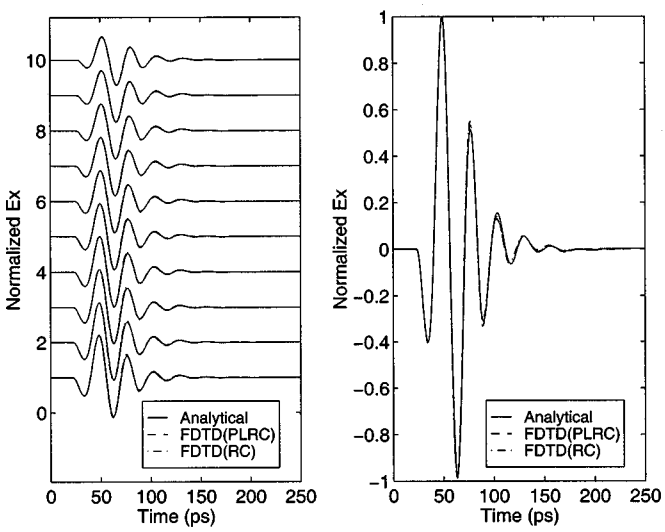

Fig. 6. Same as Fig. 3 except for a plasma sphere in the free-space.

where $s = -i\omega$ and s_q and Γ_q are the complex poles and the corresponding residues. Then the corresponding time-domain susceptibility functions can be written as

$$\chi(t) = \sum_{q=1}^{N} \mathrm{Re}[\hat{\chi}_q(t)] = \sum_{q=1}^{N} \mathrm{Re}[R_q e^{s_q t} U(t)] \tag{12}$$

where $U(t)$ is the unit step function. In (12), $N = M$, $R_q = \Gamma_q$ when all s_q, and Γ_q are real; and $N = M/2$, $R_q = 2\Gamma_q$ when there are $M/2$ complex–conjugate pole pairs (such as Lorentz media) which satisfy $\Gamma_q(s_q) = \Gamma_q^*(s_q^*)$ since $\chi(t)$ is a real function. Note that when s_q and Γ_q are real, $\hat{\chi}_q$ and all other derived functions are also real.

To simplify (10), we first introduce a unified linear approximation to $\mathbf{E}(t)$ over the time interval $t \in [m\triangle t, (m+1)\triangle t]$ as follows,

$$\mathbf{E}(t) \approx \mathbf{E}(m+1) + K_a \frac{[\mathbf{E}(m+1) - \mathbf{E}(m)]}{\triangle t}[t - (m+1)\triangle t]. \tag{13}$$

It is noted that (13) corresponds the RC [2] when $K_a = 0$ and to the PLRC [6] when $K_a = 1$. Combining these two approximation in the form of (13) is convenient for us to compare the numerical accuracy of RC and PLRC approaches in a consistent way.

Using (12) and the unified approximation (13), the convolution integral in (10) is then transformed into a discrete convolution summation

$$\mathbf{D}(n) = \epsilon_0\epsilon_\infty \mathbf{E}(n) + \epsilon_0 \sum_{q=1}^{N} \sum_{m=0}^{n-1} \mathrm{Re}\{\mathbf{E}(n-m)\hat{\chi}_q(m) + [\mathbf{E}(n-m-1) - \mathbf{E}(n-m)]\hat{\xi}_q(m)\} \tag{14}$$

where

$$\hat{\chi}_q(m) = \int_{m\triangle t}^{(m+1)\triangle t} \hat{\chi}_q(\tau)\, d\tau \tag{15}$$

$$\hat{\xi}_q(m) = \frac{K_a}{\triangle t} \int_{m\triangle t}^{(m+1)\triangle t} (\tau - m\triangle t)\hat{\chi}_q(\tau)\, d\tau. \tag{16}$$

It can be shown that

$$\hat{\chi}_q(m) = \hat{\chi}_q(0) e^{s_q m\triangle t}, \quad \hat{\xi}_q(m) = \hat{\xi}_q(0) e^{s_q m\triangle t} \tag{17}$$

and

$$\hat{\chi}(0) = \begin{cases} R_q\triangle t, & \text{for } s_q = 0 \\ \dfrac{R_q}{s_q}(e^{s_q\triangle t} - 1), & \text{for } s_q \neq 0 \end{cases} \tag{18}$$

$$\hat{\xi}_q(0) = \begin{cases} \dfrac{K_a R_q \triangle t}{2}, & \text{for } s_q = 0 \\ \dfrac{K_a R_q}{\triangle t s_q^2}[1 - (1 - s_q\triangle t)e^{s_q\triangle t}], & \text{for } s_q \neq 0. \end{cases} \tag{19}$$

Obviously, because of limited computer memory, the direct evaluation of (14) in the FDTD implementation is impracticable. Similar to [2] and [6], we introduce an auxiliary function $\mathbf{\Psi}_q(n)$ so that

$$\mathbf{\Psi}_q(n) = \sum_{m=0}^{n-1} \{[\hat{\chi}_q(0) - \hat{\xi}_q(0)]\mathbf{E}(n-m) + \hat{\xi}_q(0)\mathbf{E}(n-m-1)\} e^{s_q m\triangle t}. \tag{20}$$

Then (14) can be written as

$$\mathbf{D}(n) = \epsilon_0\epsilon_\infty \mathbf{E}(n) + \epsilon_0 \sum_{q=1}^{N} \mathrm{Re}[\mathbf{\Psi}_q(n)]. \tag{21}$$

From definition (20), a recursion relation for $\mathbf{\Psi}_q(n)$ is readily derived by using the following procedure:

$$\mathbf{\Psi}_q(n+1) = [\hat{\chi}_q(0) - \hat{\xi}_q(0)]\mathbf{E}(n+1) + \hat{\xi}_q(0)\mathbf{E}(n) + \sum_{m=1}^{n} \{[\hat{\chi}_q(0) - \hat{\xi}_q(0)]\mathbf{E}(n+1-m)$$

$$
\begin{aligned}
&+\hat{\xi}_q(0)\mathbf{E}(n-m)\}e^{s_q m\triangle t}\\
&=[\hat{\chi}_q(0)-\hat{\xi}_q(0)]\mathbf{E}(n+1)+\hat{\xi}_q(0)\mathbf{E}(n)\\
&+\sum_{m=0}^{n-1}\{[\hat{\chi}_q(0)-\hat{\xi}_q(0)]\mathbf{E}(n-m)\\
&+\hat{\xi}_q(0)\mathbf{E}(n-m-1)\}e^{s_q(m+1)\triangle t} \qquad (22)
\end{aligned}
$$

that is

$$
\begin{aligned}
\mathbf{\Psi}_q(n+1)&=[\hat{\chi}_q(0)-\hat{\xi}_q(0)]\mathbf{E}(n+1)\\
&+\hat{\xi}_q(0)\mathbf{E}(n)+\mathbf{\Psi}_q(n)e^{s_q\triangle t}. \qquad (23)
\end{aligned}
$$

Substituting (23) into (21), we find

$$
\begin{aligned}
\mathbf{D}(n+1)&=\epsilon_0\left\{\epsilon_\infty+\sum_{q=1}^{N}\mathrm{Re}[\hat{\chi}_q(0)-\hat{\xi}_q(0)]\right\}\mathbf{E}(n+1)\\
&+\epsilon_0\sum_{q=1}^{N}\mathrm{Re}[\hat{\xi}_q(0)]\mathbf{E}(n)+\epsilon_0\sum_{p=1}^{N}\mathrm{Re}[\mathbf{\Psi}_q(n)e^{s_q\triangle t}]. \qquad (24)
\end{aligned}
$$

This completes the derivation of the recursive convolution formulation for general dispersive media. Before applying the RC and PLRC approaches, a set of R_q and s_q need to be determined for a given medium. These parameters for some common dispersive media are listed below.

1) Debye media:

$$\chi(\omega)=(\epsilon_s-\epsilon_\infty)\sum_{q=1}^{N}\frac{G_q}{1-i\omega\tau_q} \qquad (25)$$

$$\chi(t)=(\epsilon_s-\epsilon_\infty)\sum_{q=1}^{N}\frac{G_q e^{-t/\tau_q}}{\tau_q}U(t) \qquad (26)$$

$$R_q=\frac{(\epsilon_s-\epsilon_\infty)G_q}{\tau_q},\quad s_q=-\frac{1}{\tau_q} \qquad (27)$$

where ϵ_s is the relative static permittivity, τ_q is the Debye relaxation time constant, and G_q is the pole amplitude.

2) Unmagnetized plasma:

$$\chi(\omega)=-\frac{\omega_p^2}{\omega(\omega+i\nu_c)} \qquad (28)$$

$$\chi(t)=\frac{\omega_p^2}{\nu_c}(1-e^{-\nu_c t})U(t) \qquad (29)$$

$$R_1=-R_2=\frac{\omega_p^2}{\nu_c},\quad s_1=0,\quad s_2=-\nu_c \qquad (30)$$

where ν_c is the collision frequency, and ω_p is the angular plasma frequency.

3) Lorentz media:

$$\chi(\omega)=(\epsilon_s-\epsilon_\infty)\sum_{q=1}^{N}\frac{G_q\omega_q^2}{\omega_q^2-2i\omega\delta_q-\omega^2} \qquad (31)$$

TABLE III
PARAMETERS FOR DEBYE MEDIA.

Medium I	Medium II
$\epsilon_\infty=3$	$\epsilon_\infty=3.7677$
$\epsilon_s=4.5$	$\epsilon_s=20.2677$
$\tau_1=6.4\times10^{-10}$ s	$\tau_1=1.1614\times10^{-11}$ s
$G_1=1$	$G_1=1$
$\sigma=0.005$ S/m	$\sigma=0.1165$ S/m

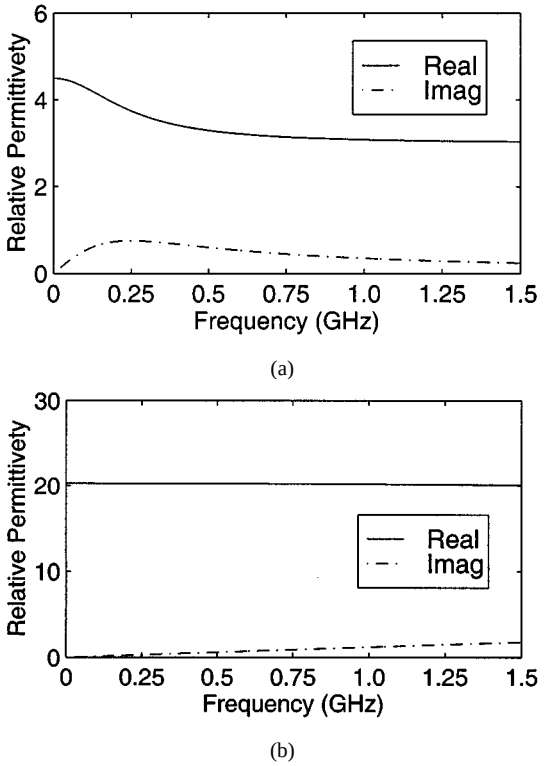

(a)

(b)

Fig. 7. Complex permittivity of Debye media I (a) and II (b).

$$\chi(t)=\sum_{q=1}^{N}\frac{(\epsilon_s-\epsilon_\infty)G_q\omega_q^2}{\sqrt{\omega_q^2-\delta_q^2}}e^{-\delta_q t}\sin\left(\sqrt{\omega_q^2-\delta_q^2}\,t\right)U(t) \qquad (32)$$

$$
\begin{aligned}
R_q&=\frac{(\epsilon_s-\epsilon_\infty)G_q\omega_q^2}{\sqrt{\omega_q^2-\delta_q^2}},\\
s_q&=-\delta_q-i\left(\frac{\pi}{2}-\sqrt{\omega_q^2-\delta_q^2}\right) \qquad (33)
\end{aligned}
$$

where δ_q is the damping constant, ω_q is the resonant angular frequency, and G_q is the normalized expansion coefficient.

It is worth pointing out that for an arbitrary linear dispersive medium, when the discrete spectral magnitude data for the susceptibility are available, the frequency-domain Prony method (FDPM) can be used to find directly the poles s_q

and residues R_q [39]. Therefore, for an arbitrary dispersive medium there is no need to fit the dispersive relation with Debye or Lorentz models.

C. Discretization

With the help of the recursive convolution equations (21), (23), and (24), we can proceed to solve Maxwell's equations by using the Yee's algorithm to discretize the split equations (6) and (7). As in the standard Yee's algorithm, the central differencing is used for both spatial and temporal derivatives. Furthermore, the second and third terms on the left-hand side of (7) require the averaging of their values at $t = n\Delta t$ and $t = (n+1)\Delta t$ since $\mathbf{E}$ is not evaluated at $t = (n+1/2)\Delta t$. We obtain

$$\left(\frac{a_\eta}{\Delta t}+\frac{\omega_\eta}{2}\right)\mathbf{H}^{(\eta)}\left(n+\frac{1}{2}\right)-\left(\frac{a_\eta}{\Delta t}-\frac{\omega_\eta}{2}\right)\mathbf{H}^{(\eta)}\left(n-\frac{1}{2}\right) =-\frac{\partial}{\partial\eta}[\hat{\eta}\times\mathbf{E}(n)]-\mathbf{M}^{(\eta)}(n) \tag{34}$$

and

$$\left(\frac{a_\eta}{\Delta t}+\frac{\omega_\eta}{2}\right)\mathbf{D}^{(\eta)}(n+1)+\left(\frac{a_\eta}{\Delta t}-\frac{\omega_\eta}{2}\right)\mathbf{D}^{(\eta)}(n) +\frac{a_\eta\sigma}{2}[\mathbf{E}^{(\eta)}(n+1)+\mathbf{E}^{(\eta)}(n)] +\omega_\eta\sigma\int_{-\infty}^{(n+1/2)\Delta t}\mathbf{E}^{(\eta)}(\tau)\,d\tau =\frac{\partial}{\partial\eta}\left[\hat{\eta}\times\mathbf{H}\left(n+\frac{1}{2}\right)\right]-\mathbf{J}^{(\eta)}\left(n+\frac{1}{2}\right). \tag{35}$$

Note that (34) remains the same as that for a nondispersive medium. Substituting (21) and (24) into (35), we have

$$c_1^{(\eta)}\mathbf{E}^{(\eta)}(n+1)=\frac{\partial}{\partial\eta}\left[\hat{\eta}\times\mathbf{H}\left(n+\frac{1}{2}\right)\right] +\mathbf{\Phi}^{(\eta)}(n)+c_0^{(\eta)}\mathbf{E}^{(\eta)}(n) -\sigma\omega_\eta\Delta t\mathbf{E}_I^{(\eta)}(n)-\mathbf{J}^{(\eta)}\left(n+\frac{1}{2}\right) \tag{36}$$

where

$$\mathbf{\Phi}^{(\eta)}(n)=\epsilon_0\sum_{q=1}^{N}\mathrm{Re}\left\{\left[\left(\frac{a_\eta}{\Delta t}-\frac{\omega_\eta}{2}\right) -\left(\frac{a_\eta}{\Delta t}+\frac{\omega_\eta}{2}\right)e^{-s_q\Delta t}\right]\mathbf{\Psi}_q^{(\eta)}(n)\right\} \tag{37}$$

$$\mathbf{E}_I^{(\eta)}(n)=\mathbf{E}_I^{(\eta)}(n-1)+\frac{7}{8}\mathbf{E}^{(\eta)}(n)+\frac{1}{8}\mathbf{E}^{(\eta)}(n-1) \tag{38}$$

and

$$c_0^{(\eta)}=\left(\frac{a_\eta}{\Delta t}-\frac{\omega_\eta}{2}\right)\epsilon_0\epsilon_\infty -\frac{a_\eta\sigma}{2}-\left(\frac{a_\eta}{\Delta t}+\frac{\omega_\eta}{2}\right)\epsilon_0\sum_{q=1}^{N}\mathrm{Re}[\hat{\xi}_q(0)] \tag{39}$$

and

$$c_1^{(\eta)}=\frac{\sigma}{2}\left[a_\eta+\frac{\omega_\eta\Delta t}{4}\right]+\left(\frac{a_\eta}{\Delta t}+\frac{\omega_\eta}{2}\right) \times\epsilon_0\left\{\epsilon_\infty+\sum_{q=1}^{N}\mathrm{Re}[\hat{\chi}_q(0)-\hat{\xi}_q(0)]\right\}. \tag{40}$$

Equations (34), (36)–(38), together with (23), form the FDTD time-stepping equations.

Note that when updating $\mathbf{E}$ field, it appears that both $\mathbf{E}(n)$ and $\mathbf{E}(n-1)$ are needed in (23) and (38). The storage requirement of $\mathbf{E}(n-1)$, actually, can be avoided by means of a temporary variable [6]. In practice, because $\mathbf{E}, \mathbf{\Phi}$ and $\mathbf{\Psi}$ are zero at $t = 0$ due to the causality, we can first update $\mathbf{E}$ using (36) with $\mathbf{E}(n-1)$ stored in the temporary variable, then update $\mathbf{E}_I, \mathbf{\Phi}_q$ and $\mathbf{\Psi}_q$ from $\mathbf{E}(n-1)$ and $\mathbf{E}(n)$ using (23), (37) and (38). Hence, the algorithm requires storage for $\mathbf{E}^{(\eta)}, \mathbf{H}^{(\eta)}, \mathbf{E}_I^{(\eta)}$, and $\mathbf{\Psi}_q^{(\eta)}$, each with six components in the PML formulation. While $\mathbf{E}_I^{(\eta)}$ is needed because of the nonzero conductivity, $\mathbf{\Psi}_q^{(\eta)}$ results from the frequency dispersion in the medium. Moreover, in general, a complex array $\mathbf{\Psi}_q^{(\eta)}$ (except for Debye media and unmagnetized plasma where it is a real array) is needed for each q, making the total storage requirement for $\mathbf{\Psi}^{(\eta)}$ proportional to the number of poles in dispersive media.

III. Numerical Results

Based on the above algorithm, a 3-D FDTD Fortran program is developed. For parallel computation, the PML equations are applied to both the interior region and the boundary region. Ten cells of PML's with a quadratic profile are used outside the region of interest as the ABC in all computations.

In following examples, an electric dipole oriented in $\hat{x}$ direction is used as a source, and the field component E_x is measured at a series of receiver locations. The time function of the source is the first derivative of the Blackman–Harris window function [37]. The central frequency of this function is defined as $f_c = 1.55/T$ where T is the duration of the source function.

A. Validation

First, we validate the algorithm for various nondispersive media by letting the electric susceptibility or the corresponding parameters go to zero. The results show an excellent agreement with those of [37].

To further validate the algorithm, we consider: 1) a homogeneous dispersive medium and 2) a dispersive sphere embedded in another dispersive or nondispersive background medium. Analytical solutions are available for a dipole source in both cases. Three types of media, i.e., Lorentz media, unmagnetized plasma, and Debye media, are under consideration. In these examples, the source is located at the origin and the E_x component at ten locations is displayed. The field is normalized with respect to the peak value at the fourth receiver. In the FDTD calculation, the computation domain is divided into 64 $\times$ 64 $\times$ 64 cells. The FDTD results are compared with the analytical solutions. However, because of limited space, only some typical results are given below.

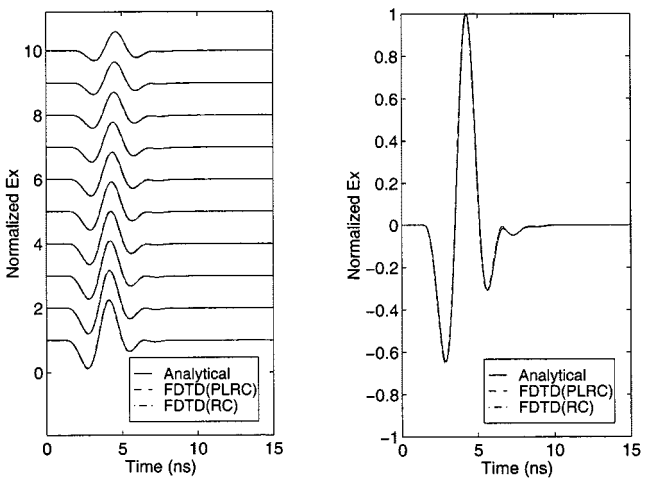

Fig. 8. Same as Fig. 3 except for a Debye sphere (medium I) in homogeneous Debye medium II. (a) The E_x component at the array of receivers. (b) The E_x component at the fourth receiver.

1) Lorentz Media: Table I gives the parameters of two Lorentz media whose real and imaginary parts of the relative complex permittivities are shown in Fig. 1. Significant dispersion are observed for both media. The central frequency of the source is 10 MHz. The spatial and temporal cell sizes are $\Delta x = \Delta y = \Delta z = 0.25$ m, $\Delta t = 0.25$ ns. The E_x field component are sampled at ten locations $x_i = 2 + 0.25 \times (i-1)$; $(y_i, z_i) = (0, 5)$ m $(i = 1, \cdots, 10)$.

Fig. 2 shows the E_x component at the fourth receiver in a homogeneous Lorentz medium I in Table I. The FDTD (RC and PLRC) results both agree well with the analytical solution.

To illustrate the PML performance, we compare this $64 \times 64 \times 64$ case with a reference case (no reflection present within the time window) to obtain the relative reflection error introduced by the PML boundary. The source is located at the center of the grid, and a receiver array is located at $(i, 16, 0)$ $(i = 10, 11, \cdots, 53)$. The typical reflection power error is below -60 dB as shown in Fig. 3.

Fig. 4(a) and (b) show the E_x distribution of a Lorentz sphere (Medium II) of radius 4 m in a homogeneous Lorentz medium (medium I) at the same receiver array and the fourth receiver, respectively. Again, the FDTD (RC and PLRC) results agree well with the analytical solutions for the array in Fig. 4(a) and for the fourth receiver in Fig. 4(b).

2) Unmagnetized Plasma: Table II gives the parameters of an unmagnetized plasma and Fig. 5 shows its frequency domain permittivity. The central frequency of the source is 25 GHz. The spatial and temporal cell sizes are $\Delta x = \Delta y = \Delta z = 0.3125$ mm, $\Delta t = 0.125$ ps. A receiver array is located at $x_i = 2.5 + 0.3125 \times (i-1)$; $(y_i, z_i) = (0, 6.25)$ mm $(i = 1, \cdots, 10)$. Fig. 6 compares the FDTD (RC and PLRC) results with the analytical solutions for a homogeneous plasma sphere in the free-space.

3) Debye Media: Fig.7 shows the frequency-domain permittivity for the two Debye media listed in Table III. The central frequency of the source is 300 MHz. The spatial and temporal cell sizes are $\Delta x = \Delta y = \Delta z = 0.781\,25$ cm, $\Delta t = 20$ ps. A receiver array is located at $x_i = 6.25 + 0.781\,25 \times (i-1)$; $(y_i, z_i) = (0, 15.625)$ cm $(i = 1, \cdots, 10)$. Fig. 8 shows the numerical (RC and PLRC) results and analytical solutions for a Debye medium sphere (medium I) of radius 12.5 cm in another homogeneous Debye medium (medium II).

4) A Note on the RC and PLRC Approaches: In the above examples, both RC and PLRC results display excellent agreement with the analytical solutions. This is different from the conclusion in literature. (Interestingly, this important observation was independently reported in two conference papers [43] and [44] after this paper was submitted.) Comparing our time-stepping equations in the previous section with the corresponding equations in the original RC and PLRC algorithms [2]–[6], one notes that the latter does not use the correct time position for the $\mathbf{E}$ field in Ampere's law. Specifically, [2]–[6] use $(n+1)\Delta t$ rather than $(n+1/2)\Delta t$, causing a larger error. In fact, since the temporal discretization is always much smaller than the spatial discretization because of the stability requirement (i.e., $c\Delta t \leq \Delta x/\sqrt{3}$), it is not expected to improve significantly the results by introducing a linear approximation to replace a constant approximation within each time step, provided that the implementation is correct.

It is worthwhile to mention that the RC approach requires less computation time than the PLRC approach, although both have the same storage requirement in the scheme presented above.

B. Applications

To demonstrate the effectiveness of the algorithm, we consider several applications in ground-penetrating radar. The earth is modeled by Debye dispersive media in all examples. For clarity, only the scattered fields obtained by subtracting the fields in the absence of buried objects from the total fields are shown. Except for the monostatic measurement, in these examples the sources are located on the air–ground interface at $(x, y) = (0, 0)$ and the receivers are located on the same interface along x-axis. The computational region is divided into either $200 \times 64 \times 64$ cells or $128 \times 64 \times 64$ cells.

1) Mine-Like Objects: As an application of the shallow subsurface object detection, we consider two mine-like objects: one is a disk of 5 cm in radius and 5 cm in height and another is a spherical cap of 5 cm in radius and 4 cm in height; both are buried in a Debye dispersive half-space. The depths from the top of the disk and cap to the ground surface is 3 and 5 cm, respectively. The disk is dielectric with $\epsilon_r = 4$ and the cap is a perfect conductor. Both buried objects are nondispersive. The electrical parameters of the earth are taken from the measured data [8] using a least-square fitting procedure. The measured effective electrical parameters of the earth are shown in Fig. 9(a) and (b). The relation between the effective electrical parameters and the complex permittivity is given by [8], [40]

$$\epsilon_e(\omega) = \epsilon_r'(\omega)\epsilon_0 \tag{41}$$

$$\sigma_e(\omega) = \sigma + \omega\epsilon_r''(\omega)\epsilon_0 \tag{42}$$

where ϵ_r' and ϵ_r'' are the real and imaginary parts of the relative complex permittivity, respectively. A first-order Debye model is chosen to fit the measured data. The parameters obtained by the

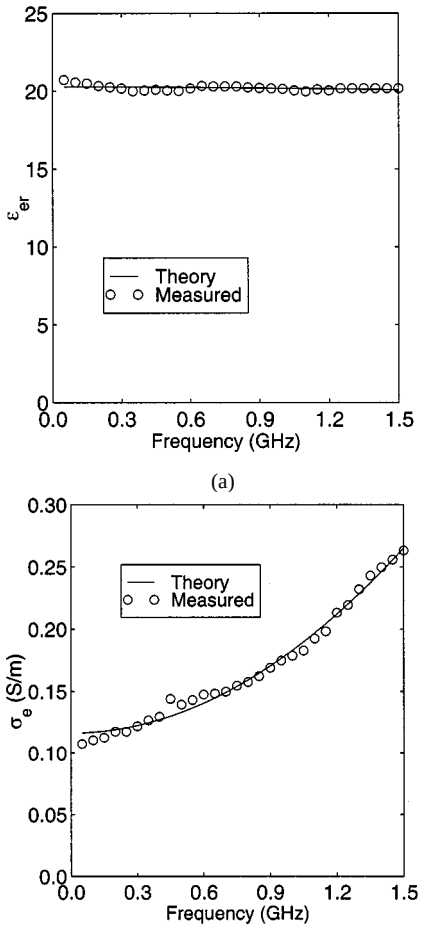

Fig. 9. Frequency-domain relative permittivity and conductivity of Debye medium II. (a) Effective relative permittivity. (b) Effective conductivity.

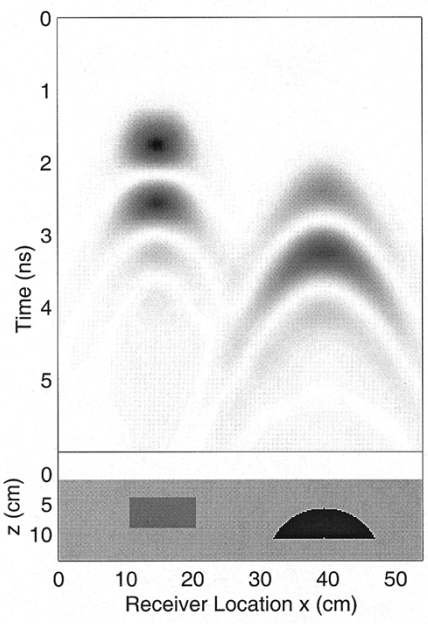

Fig. 10. The backscattered E_x field distribution of two mine-like objects buried in a Debye medium half-space.

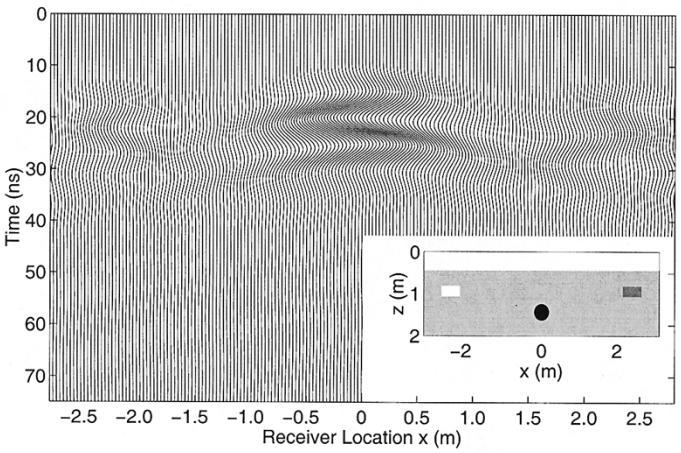

Fig. 11. Scattered E_x waveforms of two rectangular cylinders and a sphere buried in a Debye medium half-space.

least-squire fitting are given in Table III (medium II). The fitted curves are compared with the measured data in Fig. 9, and the corresponding frequency-domain complex relative permittivity is shown in Fig. 7. The central frequency of the source function is $f_c = 500$ MHz. Monostatic measurements are made at 181 source/receiver stations located on the ground surface. The backscattered fields from the two disks are shown in grey-level in Fig. 10.

2) Cylinders and a Sphere: Next, we consider two rectangular cylinders and a PEC sphere buried in a half-space of Debye medium I. The cylinders are air and Debye medium II, respectively. The central frequency of the source is 80 MHz, and the scattered E_x waveforms at 181 receiver locations are displayed in Fig. 11. As expected, the scattered field is dominated by that from the PEC sphere.

3) A Curved Interface: Finally, we consider the mapping of a curved interface by a ground-penetrating radar. The geometry of the problem is shown in Fig. 12. The upper, middle, and lower media are air, Debye medium I, and Debye medium II, respectively. The central frequency of the source is 80 MHz, and the scattered E_x waveforms recorded at 109 locations are shown in Fig. 12.

In the above application examples, the scattered fields from the buried objects or layers are clearly displayed. For the last problem with a curved interface, other ABC's will become unstable as soon as the waves propagate to the boundary. The PML ABC provides an unparalleled advantage in this aspect.

IV. Conclusion

We present a 3-D FDTD algorithm with the PML ABC for general inhomogeneous, dispersive, conductive media. The modified time-domain Maxwell's equations for dispersive media are expressed in terms of coordinate-stretching variables.

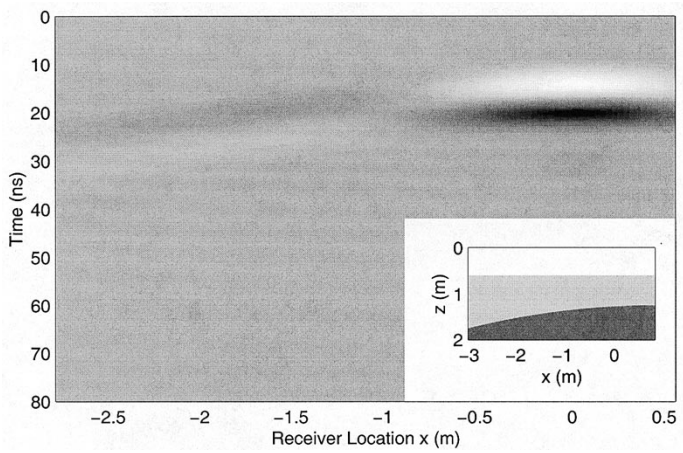

Fig. 12. The scattered E_x field distribution of a three-layer medium with a curved interface.

A unified formulation is developed to include RC and PLRC for arbitrary dispersive media. We validated the algorithm for both homogeneous dispersive media and a dispersive sphere in another dispersive or nondispersive background medium for three typical kinds of dispersive media, i.e., Lorentz medium, unmagnetized plasma, and Debye medium. Excellent agreement between the FDTD results and analytical solutions is obtained for all cases. We observed that even with the RC approach, the FDTD results are highly accurate. This can be attributed to the fact that the temporal discretization is always much smaller than the spatial discretization because of the stability requirement. Several applications are demonstrated for ground-penetrating radar detection of mine-like objects, cylinders, and a sphere buried in a dispersive half-space. Furthermore, a problem with a curved interface is simulated. The algorithm is ideal for parallel computation since the same code is shared both in the interior region and the outer matched layers. Because of their generality, the algorithm and computer program developed can be used to model biological materials, artificial dielectrics, optical materials, and other dispersive media.

ACKNOWLEDGMENT

The authors would like to thank Drs. D. Womble and S. Hutchinson of Sandia National Laboratories for the suggestions leading to this research.

REFERENCES

[1] K. S. Yee, "Numerical solution of initial boundary value problems involving Maxwell's equations in isotropic media," *IEEE Trans. Antennas Propagat.*, vol. AP-14, pp. 302–307, May 1966.

[2] R. Luebbers, F. P. Hunsberger, K. Kunz, R. Standler, and M. Schneider, "A frequency-dependent finite difference time domain formulation for dispersive materials," *IEEE Trans. Electromagn. Compat.*, vol. 32, pp. 222–227, Aug. 1990.

[3] R. J. Luebbers, F. P. Hunsberger, and K. Kunz, "A frequency-dependent finite-difference time-domain formulation for transient propagation in plasma," *IEEE Trans. Antennas Propagat.*, vol. 39, pp. 29–39, Jan. 1991.

[4] R. J. Luebbers and F. P. Hunsberger, "FDTD for Nth-order dispersive media," *IEEE Trans. Antennas Propagat.*, vol. 40, pp. 1297–1301, Nov. 1992.

[5] R. J. Luebbers, D. Steich, and K. Kunz, "FDTD calculation of scattering from frequency-dependent materials," *IEEE Trans. Antennas Propagat.*, vol. 41, pp. 1249–1257, Sept. 1993.

[6] D. F. Kelley and R. J. Luebbers, "Piecewise linear recursive convolution for dispersive media using FDTD," *IEEE Trans. Antennas Propagat.*, vol. 44, pp. 792–797, June 1996.

[7] M. D. Bui, S. S. Stuchly, and G. I. Costache, "Propagation of transients in dispersive dielectric media," *IEEE Trans. Microwave Theory Tech.*, vol. 39, pp. 1165–1171, July 1991.

[8] J. M. Bourgeois and G. S. Smith, "A full three-dimensional simulation of a ground-penetrating radar: FDTD theory compared with experiment," *IEEE Trans. Geosci. Remote Sensing*, vol. 34, pp. 36–44, Jan. 1996.

[9] T. Kashiwa and I. Fukai, "A treatment by FDTD method of dispersive characteristics associated with electronic polarization," *Microwave Opt. Tech. Lett.*, vol. 3, pp. 203–205, 1990.

[10] R. M. Joseph, S. C. Hagness, and A. Taflove, "Direct time integration of Maxwell's equations in linear dispersive media with absorption for scattering and propagation of femtosecond electromagnetic pulse," *Opt. Lett.*, vol. 16, pp. 1412–1414, Sept. 1991.

[11] O. P. Gandhi, B.-Q. Gao, and J.-Y. Chen, "A frequency-dependent finite-difference time-domain formulation for general dispersive media," *IEEE Trans. Microwave Theory Tech.*, vol. 41, pp. 658–664, Apr. 1993.

[12] J. L. Young, "Propagation in linear dispersive media: Finite difference time-domain methodologies," *IEEE Trans. Antennas Propagat.*, vol. 43, pp. 422–426, Apr. 1995.

[13] A. Taflove, *Computational Electromagnetics: The Finite-Difference Time-Domain Method*. Boston, MA: Artech House, 1995.

[14] D. M. Sullivan, "Frequency-dependent FDTD methods using Z transforms," *IEEE Trans. Antennas Propagat.*, vol. 40, pp. 1223–1230, Oct. 1992.

[15] D. M. Sullivan, "Z-transform theory and the FDTD method," *IEEE Trans. Antennas Propagat.*, vol. 44, pp. 28–34, Jan. 1996.

[16] W. H. Weedon and C. M. Rappaport, "A general method for FDTD modeling of wave propagation in arbitrary frequency-dispersive media," *IEEE Trans. Antennas Propagat.*, vol. 45, pp. 401–410, Mar. 1997.

[17] E. L. Lindman, "'Free-space' boundary conditions for the time dependent wave equation," *J. Computat. Phys.*, vol. 18, pp. 67–78, May 1975.

[18] B. Engquist and A. Majda, "Absorbing boundary conditions for the numerical simulation of waves," *Math. Computat.*, vol. 31, pp. 629–651, July 1977.

[19] G. Mur, "Absorbing boundary conditions for the finite-difference approximation of the time-domain electromagnetic-field equations," *IEEE Trans. Electromagn. Compat.*, vol. EMC-23, pp. 377–382, Nov. 1981.

[20] Z. P. Liao, H. L. Wong, B.-P. Yang, and Y.-F. Yuan, "A transmitting boundary for transient wave analysis," *Sci. Sinica*, ser. A, vol. 27, no. 10, pp. 1063–1076, 1984.

[21] R. G. Keys, "Absorbing boundary conditions for acoustic media," *Geophys.*, vol. 50, pp. 892–902, 1985.

[22] R. L. Higdon, "Absorbing boundary conditions for difference approximations to the multi-dimensional wave equations," *Math. Computat.*, vol. 47, pp. 437–459, Oct. 1986.

[23] C. Cerjan, D. Kosloff, R. Kosloff, and M. Reshef, "A nonreflecting boundary condition for discrete acoustic and elastic wave equations," *Geophys.*, vol. 50, pp. 705–708, Apr. 1985.

[24] R. Kosloff and D. Kosloff, "Absorbing boundaries for wave propagation problems," *J. Computat. Phys.*, vol. 63, pp. 363–376, Apr. 1986.

[25] C. M. Rappaport and L. Bahrmasel, "An absorbing boundary condition based on anechoic absorber for EM scattering computation," *J. Electromagn. Waves Applicat.*, vol. 6, no. 12, pp. 1621–1634, 1992.

[26] C. M. Rappaport and T. Gürel, "Reducing the computational domain for FDTD scattering simulation using the sawtooth anechoic chamber ABC," *IEEE Trans. Magn.*, vol. 31, pp. 1546–1549, May 1995.

[27] K. K. Mei and J. Fang, "Superabsorption—A method to improve absorbing boundary conditions," *IEEE Trans. Antennas Propagat.*, vol. 40, pp. 1001–1010, Sept. 1992.

[28] K. K. Mei, R. Pous, Z. Q. Chen, Y. W. Liu, and M. Prouty, "The measured equation of invariance: A new concept in field computation," *IEEE Trans. Antennas Propagat.*, vol. 42, pp. 202–214, Mar. 1994.

[29] R. Gordon, R. Mittra, A. Glisson, and E. Michielssen, "Finite element analysis of electromagnetic scattering by complex bodies using an efficient numerical boundary condition for mesh truncation," *Electron. Lett.*, vol. 29, pp. 1102–1103, June 1993.

[30] O. M. Ramahi, "Complementary operator: A method to annihilate artificial reflections arising from the truncation of the computational domain in the partial differential equations," *IEEE Trans. Antennas Propagat.*, vol. 43, pp. 697–704, July 1995.

[31] J. R. Berenger, "A perfectly matched layer for the absorption of electromagnetic waves," *J. Computat. Phys.*, vol. 114, pp. 185–200, Oct. 1994.
[32] W. C. Chew and W. H. Weedon, "A 3-D perfectly matched medium from modified Maxwell's equation with stretched coordinates," *Microwave Opt. Tech. Lett.*, vol. 7, pp. 599–604, Sept. 1994.
[33] Z. S. Sacks, D. M. Kingsland, R. Lee, and J.-F. Lee, "A perfectly matched anisotropic absorber for use as an absorbing condition," *IEEE Trans. Antennas Propagat.*, vol. 43, pp. 1460–1463, Dec. 1995.
[34] S. D. Gedney, "An anisotropic perfectly matched layer-absorbing medium for the truncation of FDTD lattices," *IEEE Trans. Antennas Propagat.*, vol. 46, pp. 1630–1639, Dec. 1996.
[35] R. W. Ziolkowski, "Time-derivative Lorentz material model-based absorbing boundary condition," *IEEE Trans. Antennas Propagat.*, vol. 45, pp. 1530–1535, Oct. 1997.
[36] J. Fang and Z. Wu, "Generalized perfectly matched layer for the absorption of propagating and evanescent waves in lossless and lossy media," *IEEE Trans. Microwave Theory Tech.*, vol. 44, pp. 2216–2222, Dec. 1996.
[37] Q. H. Liu, "An FDTD algorithm with perfectly matched layers for conductive media," *Microwave Opt. Tech. Lett.*, vol. 14, pp. 134–137, Feb. 1997.
[38] S. D. Gedney, "An anisotropic PML absorbing media for the FDTD simulation of fields in lossy and dispersive media," *Electromagn.*, vol. 16, pp. 399–415, July/Aug. 1996.
[39] T. Uno, Y. He, and S. Adachi, "Perfectly matched layer absorbing condition for dispersive medium," *IEEE Microwave Guided Wave Lett.*, vol. 7, pp. 264–266, Sept. 1997.
[40] F. L. Teixeira, W. C. Chew, M. Straka, M. L. Oristaglio, and T. Wang, "Finite-difference time-domain simulation of ground penetrating radar on dispersive, inhomogeneous, and conductive soils," *IEEE Trans. Geosci. Remote Sensing*, vol. 36, pp. 1928–1937, Nov. 1998.
[41] J. N. Brittingham, E. K. Miller, and J. L. Wilows, "Pole extraction from real-frequency information," *Proc. IEEE*, vol. 68, pp. 263–273, Feb. 1980.
[42] R. W. P. King and G. S. Smith, *Antennas in Matter: Fundamentals, Theory, and Applications*. Cambridge, MA: MIT Press, 1981.
[43] G.-X. Fan and Q. H. Liu, "A PML-FDTD algorithm for general dispersive media," in *14th Annu. Rev. Progress Appl. Computat. Electromagn.*, Monterey, CA, Mar. 1998, pp. 655–662.
[44] J. W. Schuster and R. J. Luebbers, "An accurate FDTD algorithm for dispersive media using piecewise constant recursive convolution technique," in *IEEE Antennas Propagat. Soc. Int. Symp.*, Atlanta, GA, June 1998, pp. 2018–2021.

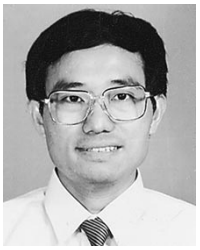

Guo-Xin Fan (M'97) received the Ph.D. degree in electrical engineering from Tsinghua University, Beijing, China, in 1995.

From 1985 to 1990, he was engaged in research as a Research Engineer and the Head of a research group on the theory and techniques on subsurface detection at the China Research Institute of Radiowave Propagation, Xinxiang, China. He was in charge of the development of the first practical ground-penetrating radar in China. From September 1995 to August 1997 he was a Postdoctoral Research Fellow in the Electromagnetics Laboratory, Department of Electrical and Computer Engineering, University of Illinois at Urbana-Champaign. From August 1997 to September 1999 he was a Postdoctoral Research Associate in the Electromagnetics Laboratory, Klipsch School of Electrical and Computer Engineering, New Mexico State University, Las Cruces. Since October 1999 he has been a Research Associate in the Department of Electrical and Computer Engineering, Duke University, Durham, NC. His research interests include computational electromagnetics, electromagnetic scattering, slotted-waveguide array antenna, subsurface target detection, and development of ground-penetrating radar.

Dr. Fan was the first winner of a Science and Technology Progress Award of the Ministry of Electronics Industry of China in 1991.

Qing Huo Liu (S'88–M'89–SM'94) received the Ph.D. degree in electrical engineering from the University of Illinois at Urbana-Champaign in 1989.

From September 1986 to December 1988, he was with the Electromagnetics Laboratory, University of Illinois at Urbana-Champaign, as a Research Assistant and from January 1989 to February 1990 as a Postdoctoral Research Associate. He was a Research Scientist and Program Leader with Schlumberger-Doll Research, Ridgefield, CT, from 1990 to 1995. From October 1995 to May 1999 he was a Faculty Member at New Mexico State University, Las Cruces. Since June 1999 he has been as Associate Professor of Electrical Engineering at Duke University, Durham, NC. He has published more than 100 papers in refereed journals and conference proceedings. His research interests include computational electromagnetics and acoustics and their applications, wave propagation in inhomogeneous media, geophysical subsurface sensing, and inverse problems.

Dr. Liu is a member of Phi Kappa Phi, Tau Beta Pi, SEG, and a full member of the U.S. National Committee of URSI Commissions B and F. He currently serves as an Associate Editor for IEEE TRANSACTIONS ON GEOSCIENCE AND REMOTE SENSING. He received a Presidential Early Career Award for Scientists and Engineerings (PECASE) from the National Science and Technology Council (NSTC) and an Early Career Research Award from the Environmental Protection Agency in 1996 and a CAREER Award from the National Science Foundation in 1997.